17. F. McCormick, *Cell* **56**, 5 (1989).
18. T. Serafini *et al.*, *ibid.*, in press.
19. G protein βγ subunits purified from bovine brain were found to contain NDK (~0.05%) as a contaminant. Hence, recombinant βγ, which was found to have less contamination (0.001%), was used for these studies. The recombinant $\beta_1\gamma_2$ was prepared as described [D. Wildman, H. Tamir, J. K. Northup, M. Dennis, in preparation]. Briefly, Sf9 cells were co-infected with baculovirus that contained β_1 and γ_2 inserts, and the membrane-associated $\beta_1\gamma_2$ dimer was purified to homogeneity.
20. Purified recombinant α subunit from G_s (α_s) (from M. P. Graziano) was prepared as described [M. P. Graziano, P. J. Casey, A. G. Gilman, *J. Biol. Chem.* **262**, 11375 (1987); M. P. Graziano, M. Freissmuth, A. G. Gilman, *ibid.* **264**, 409 (1989).]
21. We thank R. E. Parks and P. Steeg for helpful discussions; P. Steeg for nm23-H1, nm23-H2, and nm23-1 cDNAs; R. King for nm23-H1 protein; M. Dennis for the baculovirus constructs with β_1 and γ_2 inserts; and M. Graziano for purified recombinant α_2.

7 June 1991; accepted 2 August 1991

Long-Range Structure in Ribonuclease P RNA

ELIZABETH S. HAAS,* DANIEL P. MORSE,* JAMES W. BROWN,* FRANCIS J. SCHMIDT, NORMAN R. PACE†

Phylogenetic-comparative and mutational analyses were used to elucidate the structure of the catalytically active RNA component of eubacterial ribonuclease P (RNase P). In addition to the refinement and extension of known structural elements, the analyses revealed a long-range interaction that results in a second pseudoknot in the RNA. This feature strongly constrains the three-dimensional structure of RNase P RNA near the active site. Some RNase P RNAs lack this structure but contain a unique, possibly compensating, structural domain. This suggests that different RNA structures located at different positions in the sequence may have equivalent architectural functions in RNase P RNA.

RIBONUCLEASE P (RNASE P) CLEAVES precursor tRNAs to produce the mature 5′ ends; it occurs in vivo as a complex between a small protein (119 amino acids in *Escherichia coli*) and a much larger RNA (377 nucleotides). The RNA is the catalytic moiety (*1*). It is anticipated that the three-dimensional structure of the RNA determines its binding specificity and creates the catalytic site. Using two related approaches, we have identified a structure in RNase P that places constraints on three-dimensional models. Comparisons of this structure in RNase P RNAs from different organisms point to evolutionary substitution of functional domains in RNase P RNA.

We used sequence covariation (coordinated changes in nucleotide sequences) to identify base-paired elements in RNase P RNA. In a phylogenetic approach, we compared sequences of RNase P RNAs from different organisms (*2, 3*). Base-paired elements are identified by evolutionary variations that maintain the potential for Watson-Crick pairing (A-U or G-C) (*4*). In an ongoing survey of RNase P RNAs of diverse eubacteria, we have encountered covariations in sequences found to be invariant in other studies. These new sequences are from *Streptomyces bikiniensis* var. *zorbonensis* (*5*), *Deinococcus radiodurans* (*6*), and *Thermotoga maritima* (*6*). Covarying nucleotides and the consequences of their interaction in the RNase P RNA secondary-structure model are shown in Fig. 1.

Induced mutational analysis is an alternative to phylogenetic comparisons for the identification of interacting sequences. Mutations that interfere with function were introduced into the RNase P RNA, then second-site "suppressor" mutations that restore function were identified. We considered two nucleotides to form base pairs in the RNA structure if the suppressor mutation was complementary to the original mutation. At pH 6, hydroxylamine induces unidirectional G to A or C to T changes in DNA (*7*). Therefore, two induced mutagenic events can convert a G-C base pair in RNA secondary structure into an A-U pair, allowing us to identify nucleotides that interact by Watson-Crick pairing. Defective variants of RNase P RNA were screened in *E. coli* FS101. This strain produces a defective RNase P protein, causing a temperature-sensitive growth phenotype (*8*). Introduction of a high copy-number plasmid containing a functional *rnp*B gene, which encodes RNase P RNA, allows FS101 to grow at 42°C; however, a gene coding for a sufficiently defective RNase P RNA does not suppress the temperature-sensitive phenotype (*9*).

Hydroxylamine-generated mutant plasmids that did not suppress the temperature-sensitive phenotype of FS101 were isolated and sequenced (*10*) (Fig. 1B). All of these mutant genes had acquired one or two G-C to A-T transitions. Mutant plasmids that contained single lesions were subjected to a second round of hydroxylamine treatment and introduced into FS101. We identified reverted *rnp*B genes by their restoration of the ability to support the growth of FS101 at the restrictive temperature (Fig. 2).

Our comparative and mutational data revealed base pairs (Fig. 1) in helices that form two pseudoknots (*11*) in the RNA. One of the pseudoknots results from pairing of nucleotides 82 to 85 with 276 to 279 [(helix 82-85/276-279; numbering and helix nomenclature are described in (*12*)]. The mutational data show that G82 and G83 pair with C279 and C278, respectively (Fig. 1B); phylogenetic covariations support the pairing of G82 with C279, G83 with C278, and G84 with C277 (Fig. 1A). Equivalent pairings exist in all known RNase P RNAs except those of *Bacillus*, in which the structures of the contacting domains that create the pseudoknot are different.

It has been pointed out that the simultaneous occurrence of helices 12-18/336-342 and 70-73/354-357 results in the formation of a pseudoknot in RNase P RNA (*2*). Helix 70-73/354-357 has been extended by pairing G74, thought to be paired elsewhere, with C353 (*3*). It was recognized that this helix could potentially extend another three base pairs (66-68/358-360) if U69 were bulged from the helix. However, no evidence for these pairings had been encountered (*3*). Phylogenetic (Fig. 1A) and mutational (Fig. 1B) covariations now confirm the occurrence of two of the three base pairs in that extension.

The two types of sequence covariation analysis used in this study are formally equivalent, but there are important differences in the information that can be obtained. The phylogenetic approach allows the detection of base pairs only if the appropriate covariations can be found. Some variants, however, may be rare or absent in nature. In such cases, mutagenesis is required to test the pairing. Mutagenesis, on the other hand, is limited by the availability of a sensitive assay for the biological activity of the RNA. Although complementation of FS101 appears to meet this requirement, it is likely that some mutations were not detected because they did not result in a sufficiently defective enzyme or because the mutant RNA is lethal to the host at the permissive temperature. A specific limitation of hydroxylamine mutagenesis is that only G-C base pairs can be tested.

The two pseudoknots in the RNase P

E. S. Haas, J. W. Brown, N. R. Pace, Department of Biology, Indiana University, Bloomington, IN 47405. D. P. Morse and F. J. Schmidt, Department of Biochemistry, University of Missouri–Columbia, Columbia, MO 65212.

*The first three authors and laboratories contributed equivalently to the work described in this manuscript.
†To whom correspondence should be addressed.

A

Source	Helix 82-85/276-279		Helix 66-74/353-360	
Eubacterial consensus	GGGC	GCCC	AAGuCCGGG	CCCGGCUU
Thermotoga maritima	GAGC	GCUC	AAGuCCGGA	UCCGGCUU
Deinococcus radiodurans	GGGC	GCCC	AAGuCCGGG	CCCGGCUU
Streptomyces bikiniensis	GAGC	GCUC	AGGuCCGGG	CCCGGCGU
Rhodospirillum rubrum	GAAC	GUUU	AAGuCCGGG	CCCGGCUU
Agrobacterium tumefaciens	AAAU	GUUU	AAGuCCGGG	CCCGGCUU
Alcaligenes eutrophus	GGGC	GCCC	AAGuCCGGA	UCCGGCUU
Thiobacillus ferrooxidans	GGGC	GCCC	AAGuCCGGG	CCCGGCUU
γ/δ-protobacteria	GGGC	GCCC	AAGuCCGGG	CCCGGCUU
Bacillus brevis	No homolog		AAGuCCAGG	CCUGGCUU
Other *Bacillus* spp.			AAGuCCAUG	CAUGGCUU

B

Model	Mutant	Suppressor
Consistent with previous structure model	U14	A340
	A88	U241
	A91	U238
	A216	U211
	A244	U77
	A310*	U321†
	A364	U10
	A369	U5
	A74*	U353†
	U353*	A74
Extension of helix 66-74/353-360	A68	U358
	U358*	A68
New helix 82/276	U279	A82
	U278*	A83
	A83*	U278†

C

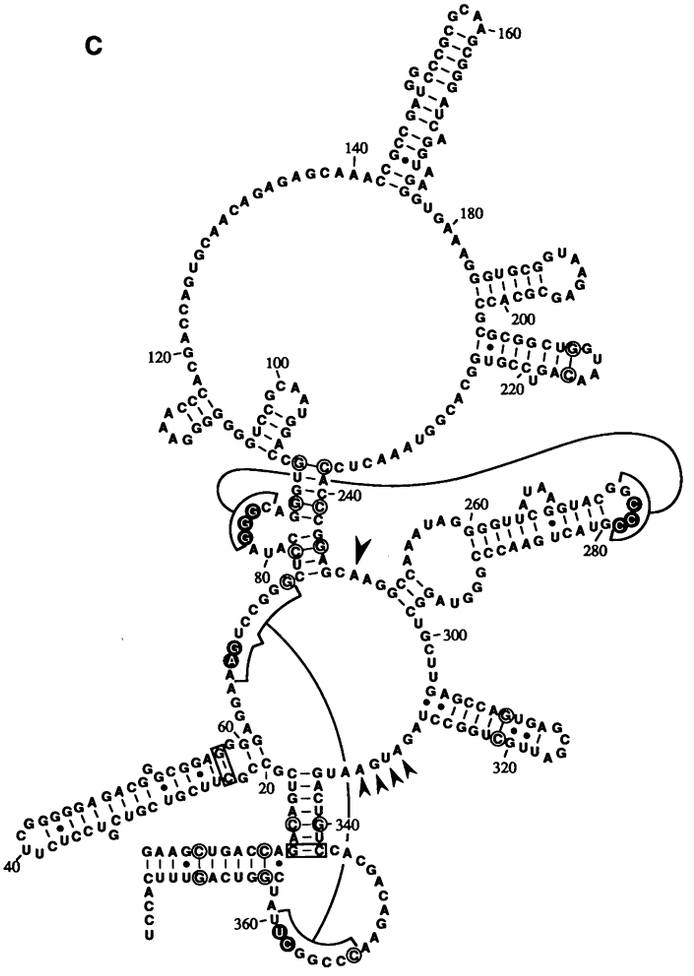

Fig. 1. Sequence covariations and revised secondary structure model of *E. coli* RNase P RNA. (**A**) Phylogenetic covariations that provide evidence for helices 82-85/276-279 and 66-74/353-360 are highlighted by black boxes. The eubacterial consensus indicates nucleotides that are conserved in at least 75% of the known eubacterial sequences. U69, shown in lower case, is bulged from the helix. Nucleotides 82 to 85 and 276 to 279 of the *Bacillus* sequences are not shown; alignment of nucleotides 82 to 85 is not meaningful because of the difference in the structure of this region (relative to those of the other RNase P RNAs), and nucleotides 276 to 279 are absent in the *Bacillus* sequences. (**B**) Mutational evidence confirms or extends the structure model as indicated. Mutants that were resolved from originally double-mutant clones are marked by asterisks. Revertants selected on MacConkey agar are marked with daggers; all other revertants were selected on NZY agar. Suppressors that restored function are shown. (**C**) The sequence of the *E. coli* RNase P RNA is drawn according to the revised structure model. The pairings indicated by brackets and lines indicate helices that complete the two pseudoknots in the secondary structure. Nucleotides in base pairs that either extend or create helices in the pseudoknots and for which new covariation evidence (either phylogenetic or mutational) is presented in this report are highlighted in black circles. Base pairs that had not been proven in earlier studies but were confirmed by phylogenetic covariations in the RNase P RNA sequences are boxed. Other base pairs known from other phylogenetic data and confirmed here by mutational analysis are highlighted in white circles. The major sites in the *E. coli* RNase P RNA that are cross-linked to 5′-azidophenacyl-tRNA ultraviolet irradiation (*13*) are indicated with arrows. Dots indicate non–Watson-Crick base pairs.

RNA impose topological and steric constraints on the structure of the molecule. The interactions probably order the central domain of RNase P RNA. This domain contains the most conserved sequences in the RNA, as well as nucleotides that are cross-linked (Fig. 1C) by a photoaffinity agent on the substrate phosphate in tRNA (*13*). Neither of the pseudoknots, however, is absolutely essential for catalytic activity in vitro. RNase P RNAs truncated at the 3′-end, including those that lack nucleotides 353 to 360, retain low amounts of enzymatic activity in vitro (*14*). Similarly, a synthetic RNase P RNA, Min 1 RNA, is catalytically active even though it lacks nucleotides 260 to 290 and thus cannot form the pseudoknot formed by helix 82-85/276-279 (*15*). However, the native RNA has a 100-fold greater affinity than does Min 1 RNA for substrate, an effect that results from the presence of nucleotides 260 to 290 (*16*).

In light of the structural importance of nucleotides 260 to 290, it is surprising that the *Bacillus* RNase P RNA lacks the corresponding nucleotides and therefore would seem to lack the pseudoknot. Nevertheless, the *Bacillus* RNA interacts with the *E. coli* protein component of RNase P in vitro (*1*) and can replace *E. coli* RNase P RNA in vivo (*17*). The functionality of the *Bacillus* RNA in the absence of the 260 to 290 helix could be explained if another structural ele-

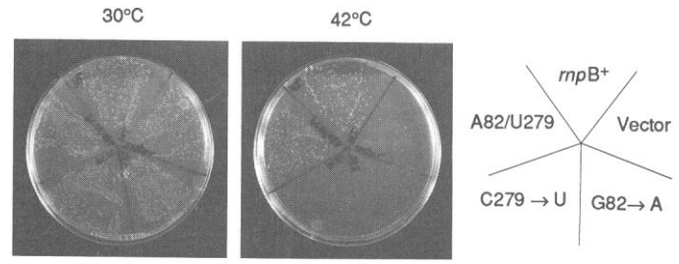

Fig. 2. Representative examples of hydroxylamine mutagenesis of RNase P RNA. RNase P activity in vivo was assayed by the ability of plasmids to allow growth of *E. coli* FS101 at 42°C. The plate at 30°C is a control. The diagram at right indicates the plasmids we used to transform FS101. Two sets of sectors on the plates show the results of control experiments in which the temperature-sensitive growth phenotype of *E. coli* FS101 was suppressed by a plasmid containing the wild-type *E. coli* RNase P RNA gene (*rnp*B$^+$) but not by a plasmid containing the cloning vector sequences only. A hydroxylamine-generated G to A transition at position 82 of the RNase P RNA gene resulted in a plasmid that did not suppress the growth defect at 42°C (G82 → A). Likewise, the C to U mutation at position 279 failed to suppress the growth defect at 42°C (C279 → U). Growth of the plasmid-containing FS101 at 42°C, however, is restored in the double-mutant containing both the G to A change at position 82 and the C to U change at position 279 (A82/U279), which are compensatory in the secondary structure of the RNA (Fig. 1).

ment could independently fulfill the function of that helix. One structural element present in the *Bacillus* RNA, but not the *E. coli* RNA, is a likely candidate for such functional replacement: a genus-specific helix at approximately the same position as the pseudoknot in the *E. coli* RNA (Fig. 3). It is possible that this helix can fulfill the function of the pseudoknot in which the 82-85/276-279 helix in the *E. coli* RNA participates. Molecular modeling indicates that the two structures could have similar three-dimensional aspects (Fig. 3). Thus, different RNA structures, located at different positions in the sequence, may have equivalent architectural functions in RNase P RNAs.

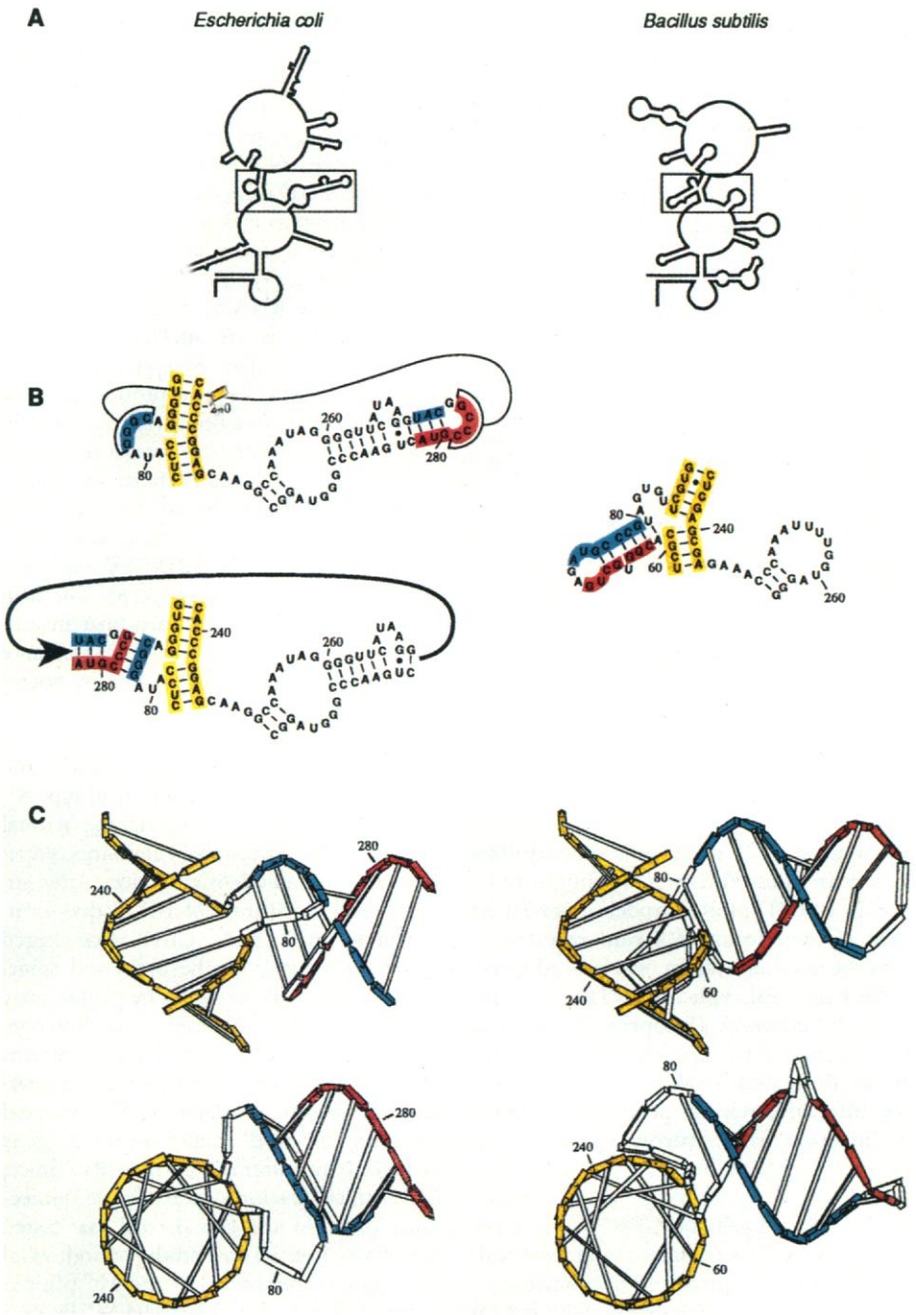

Fig. 3. Potential evolutionary substitution of functional elements. The secondary structures of the *E. coli* and *B. subtilis* RNase P RNAs are outlined in (**A**). The boxed regions include the pseudoknot in *E. coli* and the analogous region of the *B. subtilis* structure and are enlarged in (**B**). We show the pseudoknot in the *E. coli* structure as in Fig. 1, as well as disjointed to allow the direct representation of helix 82-85/276-279. Molecular "pencil-figure" models of the long-range interaction in the *E. coli* RNase P RNA and the analogous region in the *B. subtilis* RNA are shown in front and top views in (**C**). The molecular models contain only nucleotides 75 to 91, 238 to 246, and 272 to 282 in *E. coli* and 58 to 90 and 235 to 243 in *B. subtilis*; the remainder of the structures are omitted for clarity. Analogous portions of the models are colored in both (B) and (C). *Bacillus subtilis* nucleotides are numbered according to the *B. subtilis* sequence. Helices 75-78/243-246 and 87-91/238-242 in *E. coli* and the analogous helices in *B. subtilis* are modeled as coaxially stacked as are *E. coli* helices 82-85/276-279 and 272-274/280-282. G275 in *E. coli* spans the major groove of helix 82-85/276-279 as in an H-type pseudoknot (*18*). The *Bacillus*-specific helix 62 to 80 is modeled as a tetraloop-stem based on its sequence (GAGA loop) (*19*) and the known structure of a different tetraloop-containing helix (*20*). Models were constructed with Swivel 3D (Paracomp, San Francisco, California) on a Macintosh IIci computer.

REFERENCES AND NOTES

1. C. Guerrier-Takada *et al.*, *Cell* **35**, 849 (1983); N. R. Pace and D. Smith, *J. Biol. Chem.* **265**, 3587 (1990); S. Altman, *ibid.*, p. 20053.
2. B. D. James *et al.*, *Cell* **52**, 19 (1988).
3. J. W. Brown, E. S. Haas, B. D. James, D. A. Hunt, N. R. Pace, *J. Bacteriol.* **173**, 3855 (1991).
4. R. R. Gutell, B. Weiser, C. R. Woese, H. F. Noller, *Prog. Nucleic Acid Res.* **32**, 155 (1985).
5. Genomic DNA from *S. bikiniensis* var. *zorbonensis* [J. H. Coats and J. Roeser, *J. Bacteriol.* **105**, 880 (1971)] was partially cleaved with Sau 3AI, and fragments that ranged from 1 to 3 kb in length were ligated into pTZ19R [D. A. Mead *et al.*, *Protein Eng.* **1**, 67 (1986)]. The library was transformed into *E. coli* strain DW2 (*17*), and a clone supporting growth of this strain at 42°C was identified. The sequence of the RNase P RNA gene was determined by the dideoxy chain-termination method with the use of Sequenase version 2.0 (United States Biochemicals). The GenBank accession number of this sequence is M64290.
6. Restriction endonuclease digests of genomic DNAs were separated by agarose gel electrophoresis, and fractions of gels that contained RNase P RNA genes were excised on the basis of Southern blot information. DNA was recovered from gel slices by disruption with sodium iodide; and DNA was purified with glass powder [B. Vogelstein and D. Gillespie, *Proc. Natl. Acad. Sci. U.S.A.* **76**, 615 (1979)]. The size-selected DNAs were then cloned into pBluescript KS$^-$ (Stratagene) and screened by colony hybridization with the same probes used for the Southern analyses. Confirmation of potential clones was by RNase P assays of T7 and T3 RNA polymerase–generated transcripts from the clones (*3*). Plasmid DNAs were sequenced by the dideoxy chain-termination method with Sequenase version 2.0 after we generated a series of nested deletions using exonuclease III and nuclease S1 [S. Henikoff, *Gene* **28**, 351 (1984)]. We used 7-deazadeoxyguanosine triphosphate to alleviate band compression in sequencing gels. The RNase P RNA gene from *D. radiodurans* (GenBank accession number M64708), contained on a 1.8-kb Hind III–Pst I DNA fragment, was identified with the use of an oligonucleotide that contained the most conserved sequence from known RNase P RNAs (5′-GIIGAGGAAAGTCCIIGCT-3′: I is inosine) as a probe. The RNase P RNA gene from *T. maritima* (GenBank accession number M64709), contained on a 2.3-kb Hind III DNA fragment, was identified with a partially hydrolyzed antisense transcript of the *E. coli* RNase P RNA gene (*3*).
7. L. Fishbein, W. G. Flamm, H. L. Falk, *Chemical Mutagens: Environmental Effects on Biological Systems* (Academic Press, New York, 1970), pp. 27–28.
8. P. Schedl and P. Primakoff, *Proc. Natl. Acad. Sci. U.S.A.* **70**, 2091 (1973).
9. H. Motamedi, K. Lee, L. Nichols, F. J. Schmidt, *J. Mol. Biol.* **162**, 535 (1982).
10. The plasmid pTZMIKE (pTZ19R with a 1.5-kb Kpn I–Eco RI insert that contains the *E. coli* RNase P RNA gene) was reacted with hydroxylamine and dialyzed overnight against three changes of deionized water. Reaction conditions were identical to those described [R. Eichenlaub, *J. Bacteriol.* **138**, 559 (1979)]. The DNA was concentrated by ethanol precipitation and introduced into *E. coli* FS101. Transformants were selected on NZY-ampicillin [T. Maniatis, E. F. Fritsch, J. Sambrook, *Molecular*

Cloning: A Laboratory Manual (Cold Spring Harbor Laboratory, Cold Spring Harbor, NY, 1982)] plates at 30°C, and each colony was picked onto duplicate NZY-ampicillin plates for incubation at 30°C and 42°C. Plasmid DNA was purified from FS101 clones that did not grow at 42°C, and DNA was introduced into *E. coli* DH5α. Transformants were plated at 30°C and 42°C. We used DH5α, which contains the wild-type RNase P RNA gene, to ensure that failure to complement the FS101 phenotype was not the result of a temperature-sensitive plasmid function. We identified the mutations in RNase P RNA genes present on plasmids that did not complement FS101 but successfully transformed DH5α at 42°C by sequencing the genes. Mutant plasmids that did not complement FS101 were subjected to a second round of hydroxylamine mutagenesis and reintroduced into FS101. We selected revertants by plating the transformants at 42°C. Plasmid DNA from colonies that grew at 42°C were introduced again into FS101 and tested for their ability to complement the temperature-sensitive phenotype. Revertant genes were sequenced.

11. The term "pseudoknot" describes the structure that results from pairing (helix formation) between nucleotides contained in a loop and nucleotides outside of that loop. A pseudoknot, therefore, is a topological (rather than secondary or tertiary) structure composed of two equivalent helices and their interconnections [C. W. A. Pleij, K. Reitveld, L. Bosch, *Nucleic Acids Res.* **13**, 1717 (1985)].
12. Unless otherwise indicated, numbering is based on the *E. coli* sequence. Helix designations are based on the numbering of the nucleotides of each strand of the helix. For example, the helix that is formed by the pairing of nucleotides 260 to 265 with nucleotides 285 to 290 is referred to as helix 260-265/285-290.
13. A. B. Burgin and N. R. Pace, *EMBO J.* **9**, 4111 (1990).
14. C. Guerrier-Takada and S. Altman, *Cell* **45**, 177 (1986); D. S. Waugh, thesis, Indiana University (1989).
15. D. S. Waugh, C. J. Green, N. R. Pace, *Science* **244**, 1569 (1989).
16. S. C. Darr, K. Zito, N. R. Pace, unpublished data.
17. D. S. Waugh and N. R. Pace, *J. Bacteriol.* **172**, 6316 (1990).
18. C. W. A. Pleij, *Trends Biochem. Sci.* **15**, 143 (1990).
19. C. R. Woese, W. Winkler, R. R. Gutell, *Proc. Natl. Acad. Sci. U.S.A.* **87**, 8467 (1990).
20. C. Cheong, G. Varani, I. Tinoco, Jr., *Nature* **346**, 680 (1990).
21. We thank S. C. Darr and K. Zito for discussion and unpublished data, D. Hunt for technical assistance, and M. Calcutt for DNA from *S. bikiniensis*. Supported by NIH grant GM34527 (to N.R.P.), a Postdoctoral Fellowship (to J.W.B.) from Indiana University Institute for Molecular and Cellular Biology, the University of Missouri–Columbia School of Medicine and American Cancer Society grant MV 457 (to F.J.S.), and a University of Missouri–Columbia Molecular Biology Program Predoctoral Fellowship (to D.P.M.).

6 May 1991; accepted 9 July 1991

Antibody-Mediated Clearance of Alphavirus Infection from Neurons

BETH LEVINE, J. MARIE HARDWICK, BRUCE D. TRAPP, THOMAS O. CRAWFORD, ROBERT C. BOLLINGER, DIANE E. GRIFFIN*

Humoral immunity is important for protection against viral infection and neutralization of extracellular virus, but clearance of virus from infected tissues is thought to be mediated solely by cellular immunity. However, in a SCID mouse model of persistent alphavirus encephalomyelitis, adoptive transfer of hyperimmune serum resulted in clearance of infectious virus and viral RNA from the nervous system, whereas adoptive transfer of sensitized T lymphocytes had no effect on viral replication. Three monoclonal antibodies to two different epitopes on the E2 envelope glycoprotein mediated viral clearance. Treatment of alphavirus-infected primary cultured rat neurons with these monoclonal antibodies to E2 resulted in decreased viral protein synthesis, followed by gradual termination of mature infectious virion production. Thus, antibody can mediate clearance of alphavirus infection from neurons by restricting viral gene expression.

ACCORDING TO THE CLASSIC PARADIGM, the clearance of infectious virus from primary sites of replication results from major histocompatibility complex (MHC) class I–restricted lysis of virally infected cells by $CD8^+$ cytotoxic T lymphocytes. This paradigm can theoretically explain viral clearance from nonneuronal cellular targets in the central nervous system (CNS), but it cannot account for viral clearance from neurons. Neurons are not induced to express class I molecules in vivo in response to cytokine stimulation and viral infection (*1*) and therefore may escape immune recognition by virus-specific $CD8^+$ cells. Furthermore, it seems unlikely that terminally differentiated cells incapable of replication would use a cytolytic mechanism for recovery from viral infection; this hypothesis is supported by histopathologic findings in lymphocytic choriomeningitis virus infection where viral clearance from neurons occurs without evidence of cellular lysis (*2*). Thus, a non-MHC–restricted, noncytotoxic immunologic mechanism for the termination of viral infection of neurons must exist; yet the nature of such a mechanism is poorly understood.

To investigate the primary immunologic mechanism responsible for the clearance of infectious virus from neurons, we used a SCID (severe combined immunodeficient) mouse model of Sindbis virus (SV) infection. The SCID mice lack functional mature B and T lymphocytes because of a defect in T cell receptor and immunoglobulin gene rearrangement (*3*). SV is a single-stranded message-sense RNA virus that causes fatal encephalomyelitis in suckling mice and acute, clinically silent encephalomyelitis in weanling mice (*4*). It is the prototypic member of the alphavirus genus (family Togaviridae), which includes the human pathogens Eastern, Western, and Venezuelan equine encephalitis viruses. In contrast to many other neurotropic viruses that have multiple cellular targets in the CNS, SV replicates predominantly in neurons (*5, 6*). The neuronal specificity of SV ensures that investigation of the mechanism of viral clearance from neurons is not complicated by potentially different mechanisms of viral clearance from other cell populations in the CNS.

We infected 4- to 6-week-old CB17 and congenic *scid*/CB17 mice with wild-type SV (strain AR339) to determine the natural history of SV infection in immunocompetent and immunodeficient mice. After intracerebral inoculation of 10^3 plaque-forming units (pfu) of SV, CB17 mice cleared infectious virus from the brain and spinal cord in 8 days, as measured by plaque-assay titrations of freeze-thawed tissue homogenates (Fig. 1A). Clearance of infectious virus was temporally correlated with the appearance of serum antibody to SV detected by enzyme-linked immunosorbent assay (ELISA). In contrast to the CB17 mice, SCID mice developed persistent SV infections of brain and spinal cord that lasted for the entire 30-day study period; viral titers ranged between 10^4 and 10^6 pfu per gram of tissue (Fig. 1A). The SCID mice had no detectable amounts of serum antibody and no detectable T lymphocytes in the spleen, lymph nodes, or peripheral blood, as measured by flow cytometry analysis. Despite ongoing viral replication and the lack of specific humoral or cellular immune responses, there was no evidence of neurologic disease in the SCID mice.

After establishing that SCID mice develop persistent SV infections, we investigated the effect of transferred immune T lymphocytes and SV hyperimmune serum on the clearance of infectious virus from neural tissue.

B. Levine and R. C. Bollinger, Department of Medicine, Johns Hopkins University School of Medicine, Baltimore, MD 21205.
J. M. Hardwick, Departments of Neurology and Pharmacology and Molecular Sciences, Johns Hopkins University School of Medicine, Baltimore, MD 21205.
B. D. Trapp and T. O. Crawford, Department of Neurology, Johns Hopkins University School of Medicine, Baltimore, MD 21205.
D. E. Griffin, Departments of Medicine and Neurology, Johns Hopkins University School of Medicine, Baltimore, MD 21205.

*To whom correspondence should be addressed.